# Intracellular trafficking of pigeon β-very low density lipoprotein and low density lipoprotein at low and high concentrations in pigeon macrophages

**Nancy L. Jones, Jerry A. Saunders, and Revill R. Mallory**

Pathology Department, Wake Forest University School of Medicine, Winston-Salem, NC 27157

**Abstract** **Foam cell formation occurs in vitro at lipoprotein concentrations above 50 μg/ml in pigeon macrophages. Hypothetically, intracellular trafficking of lipoproteins at higher concentrations may differ from uptake of lipoproteins associated with low concentrations, revealing a separate atherogenic endocytic pathway. Macrophage intracellular trafficking of pigeon β-very low density lipoprotein (β-VLDL) and low density lipoprotein (LDL) at low concentrations (12 μg/ml) near the saturation of high affinity binding sites and high lipoprotein concentrations (50–150 μg/ml) used to induce foam cell formation were examined. Pigeon β-VLDL and LDL, differentially labeled with colloidal gold, were added simultaneously to contrast trafficking of β-VLDL, which causes in vitro foam cell formation, with LDL, which does not. The binding of lipoproteins to cell surface structures, distribution of lipoproteins in endocytic organelles, and the extent of colabeling in the endocytic organelles were determined by thin-section transmission electron microscopy. At low concentrations, the intracellular trafficking of pigeon LDL and β-VLDL was identical. At high concentrations, LDL was removed more rapidly from the plasma membrane and reached lysosomes more quickly than β-VLDL. No separate endocytic route was present at high concentrations of β-VLDL; rather, an increased residence on the plasma membrane, association with nonmicrovillar portions of the plasma membrane, and slower trafficking in organelles of coated-pit endocytosis reflected a more atherogenic trafficking pattern.**—Jones, N. L., J. A. Saunders, and R. R. Mallory. **Intracellular trafficking of pigeon β-very low density lipoprotein and low density lipoprotein at low and high concentrations in pigeon macrophages.** ***J. Lipid Res.*** **2000.** 41: **1823–1831.**

**Supplementary key words** endocytosis • foam cell formation • ultrastructure

Macrophages accumulate cholesterol and cholesteryl esters derived from plasma lipoproteins, resulting in the formation of macrophage-derived foam cells. Pigeon blood monocytes have been cultured in vitro as a model for monocyte-derived foam cells. Like human macrophages (1) they can be stimulated by endocytosis of either β-very low density lipoprotein (β-VLDL), acetylated low density lipoprotein (AcLDL) or oxidized LDL (OxLDL) to accumulate cholesteryl esters, resulting in a foam cell-like appearance (2–4). Native LDL does not cause cholesteryl ester accumulation.

Previous studies speculated that intracellular processing of lipoproteins that stimulate cholesteryl ester accumulation and subsequent foam cell formation is different from the processing of those lipoproteins that do not cause foam cell formation (5). This is the case for the modified LDLs, AcLDL and OxLDL. These lipoproteins are internalized in part by a unique endocytic route, macropinocytosis (6). Macropinocytosis is hypothesized to be an atherogenic route of internalization for modified LDL (6). However, at lipoprotein concentrations near the saturation of high affinity binding sites (<20 μg/ml), LDL and β-VLDL did not show separate endocytic pathways for nonatherogenic lipoproteins versus atherogenic lipoproteins (5). Cell fractionation has shown that LDL at higher concentrations is distributed to a different subcellular fraction than malondialdehyde-LDL and other ligands. This suggests that intracellular pathways may be dependent on the concentration of ligands (7). However, to date ultrastructural studies have examined lipoproteins only at concentrations near the saturation of the high affinity binding sites rather than examining if a separate atherogenic endocytic route is present at concentrations used to induce foam cell formation.

Another hypothesis for atherogenic trafficking of lipoproteins is delayed trafficking to lysosomes, rather than a separate endocytic pathway. In this model, the slower trafficking and retention on the plasma membrane would be associated with foam cell formation. Several

Abbreviations: ACAT, acyl-coenzyme A:cholesterol acyltransferase; AcLDL, acetylated LDL; apo, apolipoprotein; β-VLDL, β-very low density lipoprotein; HDL, high density lipoprotein; HSPG, heparan sulfate proteoglycan; LDL, low density lipoprotein; LEPT, late endosomal-prelysosomal tubular compartment; OxLDL, oxidized LDL; PBS, phosphate-buffered saline; TEM, transmission electron microscopy; STEM, surface tubules for entry into macrophages.

[1] To whom correspondence should be addressed.

studies have shown that atherogenic lipoproteins are retained on the plasma membrane surface (8–11). Fluorescently labeled β-VLDL was retained on the plasma membrane compared with LDL at 2 min (8). The retention of different subfractions of β-VLDL on the cell periphery correlated positively with the extent of acyl-coenzyme A:cholesterol acyltransferase (ACAT) stimulation. The peripheral cytoplasmic β-VLDL trafficked through surface tubules for entry into macrophages (STEM). STEMs are long tubules (>1 μm) and accessible by diffusion to small macromolecules, but they exclude larger macromolecules such as antibodies (10). Eventually, β-VLDL was delivered to perinuclear lysosomes, where fluorescence microscopy showed partial colocalization with LDL by 10 min in the central perinuclear cytoplasm. AcLDL was also shown to be retained on the plasma membrane compared with LDL (9). All these studies used lipoprotein concentrations near the saturation of the high affinity binding sites.

The present study used simultaneous labeling methodology to compare and contrast pigeon macrophage uptake of β-VLDL and LDL at the ultrastructural level. Early times of <1, 5, and 10 min were of particular interest, and therefore we examined if early temporal differences occurred during lipoprotein(s) internalization by macrophages. In addition, this study examined whether intracellular trafficking of lipoproteins at high concentrations (50–100 μg/ml), used for in vitro foam cell formation, is the same as intracellular trafficking of lipoprotein at concentrations near the saturation of high affinity binding sites.

## MATERIALS AND METHODS

### Macrophage culture and lipoproteins

White Carneau pigeon monocytes were isolated by differential centrifugation of anticoagulated blood as previously reported (12). β-VLDL (d < 1.006 g/ml) and hypercholesterolemic LDL (d < 1.080) were isolated from the plasma of hypercholesterolemic random bred White Carneau pigeons as previously described (12). The composition of pigeon β-VLDL versus LDL is 7.5 versus 22% protein, 11 versus 9% free cholesterol, 56.8 versus 37.5% cholesteryl ester, 10.8 versus 8.2% triglyceride, and 13.9 versus 23.3% phospholipid (13). The predominant apolipoproteins for pigeon LDL and β-VLDL are apolipoprotein (apo)B-100 and apoA-I, with smaller amounts of several minor unidentified apolipoproteins (14). Pigeon LDL has approximately equal concentrations of apoB-100 and apoA-I. ApoA-I is the predominant apolipoprotein for pigeon β-VLDL. For equal protein concentrations, pigeon β-VLDL has approximately half the number of particles and delivers 4.5 times the cholesterol than pigeon LDL. The lipoproteins were spot checked for the presence of endotoxin (E-Toxate kit, Sigma Chemical, St. Louis, MO) and were consistently negative between 0.05 and 0.10 ng/ml. Lipoproteins (20 μg/ml) were conjugated to colloidal gold (small gold, 16 or 21 nm; and large gold, 30 or 48 nm). On average, three to five lipoprotein particles were conjugated to each gold colloid. Sizes of gold colloids were switched to control to determine effects of the gold particle size and conjugation; no differences in trafficking over time or the extent of colabeling were seen due to the differences in the size of gold conjugates in this study or previously published studies (5, 15).

For the low concentration, lipoproteins were mixed (1:1 ratio) after gold conjugation for a final concentration of 12.5 μg/ml for each individual lipoprotein. For the high concentration, after conjugation as described above, each lipoprotein was layered over 60% sucrose and centrifuged at 1,200 *g*, overnight at 4°C. The dark pink interface of concentrated lipoprotein was collected and the volume was measured before and after dialysis with medium A to determine the final concentration of lipoprotein. Two experiments, β-VLDL and LDL, were performed at 100 μg/ml and one experiment, lipoproteins, was performed at 50 μg/ml.

### Simultaneous trafficking of lipoproteins

Macrophages were incubated with equal concentrations of β-VLDL and LDL, at either low concentrations (12.5 μg/ml) or high concentrations (50–100 μg/ml). Cells were washed twice with ice-cold phosphate-buffered saline (PBS) and then incubated with labeled lipoproteins for 2 h at 4°C. The cells were then washed twice with PBS at 4°C. Medium, prewarmed to 37°C, was added and the cells were incubated at 37°C for <1, 5, 10, 30, 60, and 120 min. Cells were then fixed with 2.5% glutaraldehyde and embedded in Spurr's for standard thin-section, transmission electron microscopy (TEM). Silver thin sections (60–80 nm) were visualized at 80 keV in a Philips (Mt. Vernon, NY) EM-400 TEM. The colloidal gold distribution was determined for organelles of macrophages: plasma membrane, clathrin-coated and noncoated pits and vesicular profiles, early endosomes, macropinosomes, spherical late endosomes, late endosomal-prelysosomal tubuloreticular compartments (LEPT), and lysosomes. Morphologies used to classify organelles are described by Jones, Reagan, and Willingham (15). Greater than 99% of the gold colloids were within the above-described organelles. The percentage of gold distribution was determined for each time point by totaling the gold labeling in each organelle for 11 micrographs (×7,000) divided by the total label in all organelles. Four low concentration experiments and three high concentration experiments were averaged.

### Analysis of colabeling

The colabeling of all organelle types, except the plasma membrane, was analyzed by the percentage of the labeled lipoprotein in the colabeled organelles. The lipoprotein in the colabeled organelles was divided by the total lipoprotein in each organelle type. Although the distribution of lipoproteins in each organelle changed with time, the percentage of lipoprotein in the colabeled organelles did not differ with time. Therefore, colabeling data were averaged for each organelle, despite time. The nonparametric Wilcoxon paired *t*-test was used to analyze significant differences between the lipoprotein pairs for each organelle. Nonparametric multiple comparisons were made by Kruskal-Wallis analysis to determine whether the colabeling of organelles was different among the six organelle types. When the null hypothesis was rejected, significant differences at the $P < 0.05$ level between organelles were determined by a nonparametric Tukey-type comparison (Instat version 3.00; GraphPad Software, San Diego, CA).

### Surface area quantification

The 10-min time points were quantified for location of lipoprotein binding. The cell surface was measured with a map wheel (PlanWheel, Scalex Corporation, Carlsbad, CA) and divided into four groups: *1*) microvilli and small membrane ruffles (<0.22-μm base width), *2*) large membrane ruf-

fles (>0.22-μm base width), *3*) smooth membrane regions, and *4*) basal surface, the side in contact with the substrate (16). Microvilli and small ruffles were grouped together because of the difficulty in separating these two structures in thin sections.

### Competition experiment for surface binding sites

Macrophages were incubated with either pigeon β-VLDL or rabbit β-VLDL conjugated to 22-nm colloidal gold at 20 μg/ml for 2 h at 4°C. A 30-fold excess of unlabeled pigeon β-VLDL, LDL, high density lipoprotein (HDL), or rabbit β-VLDL was added. Cells were washed with PBS, fixed with 2.5% glutaraldehyde, and embedded in Spurr's for standard thin-section, TEM. Silver thin sections (60–80 nm) were visualized at 80 keV in the Philips EM-400 TEM. The distribution of the surface area and percent binding of lipoproteins was determined for microvilli, membrane ruffles, smooth membrane, and basal surface for 11 micrographs (×7,000) from each condition.

## RESULTS

### Uptake of lipoproteins at high affinity (low concentration)

Overall, the time course of endocytosis at low concentration (12 μg/ml) of β-VLDL and LDL in macrophages was similar to endocytosis of LDL alone. β-VLDL and LDL maximally entered the clathrin-coated pits and vesicular profiles and early endosomes by 5 min, spherical endosomes by 10 min, LEPT by 60 min, and lysosomes by 2 h (**Fig. 1**). Approximately 70% of β-VLDL and LDL reached the lysosomes by 2 h. β-VLDL and LDL had a nearly superimposable time course through the endocytic organelles. The only difference was that, although LDL initially peaked in spherical endosomes at 10 min, similar to β-VLDL, LDL was still present at 60 min in spherical endosomes. In contrast, little β-VLDL was present in spherical endosomes at 60 min.

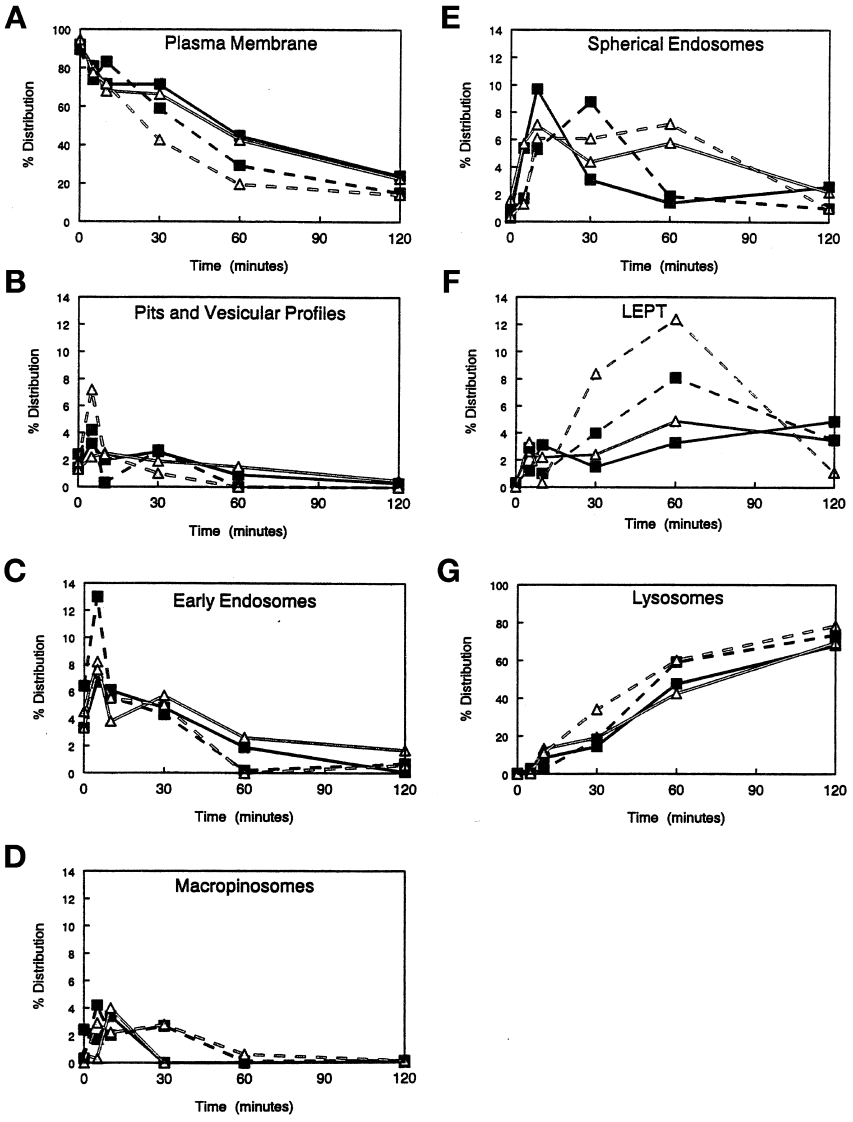


**Fig. 1.** Distribution of lipoproteins in organelles. The time course of the percentage distribution of β-VLDL and LDL is shown for the plasma membranes, pits and vesicular profiles, early endosomes, macropinosomes, spherical endosomes, LEPT, and lysosomes. Shown is the distribution over time of β-VLDL (squares) and LDL (triangles), incubated at low concentrations to examine the high affinity binding sites (solid lines) and at high concentrations to examine lipoprotein concentrations associated with foam cell formation (dashed lines).

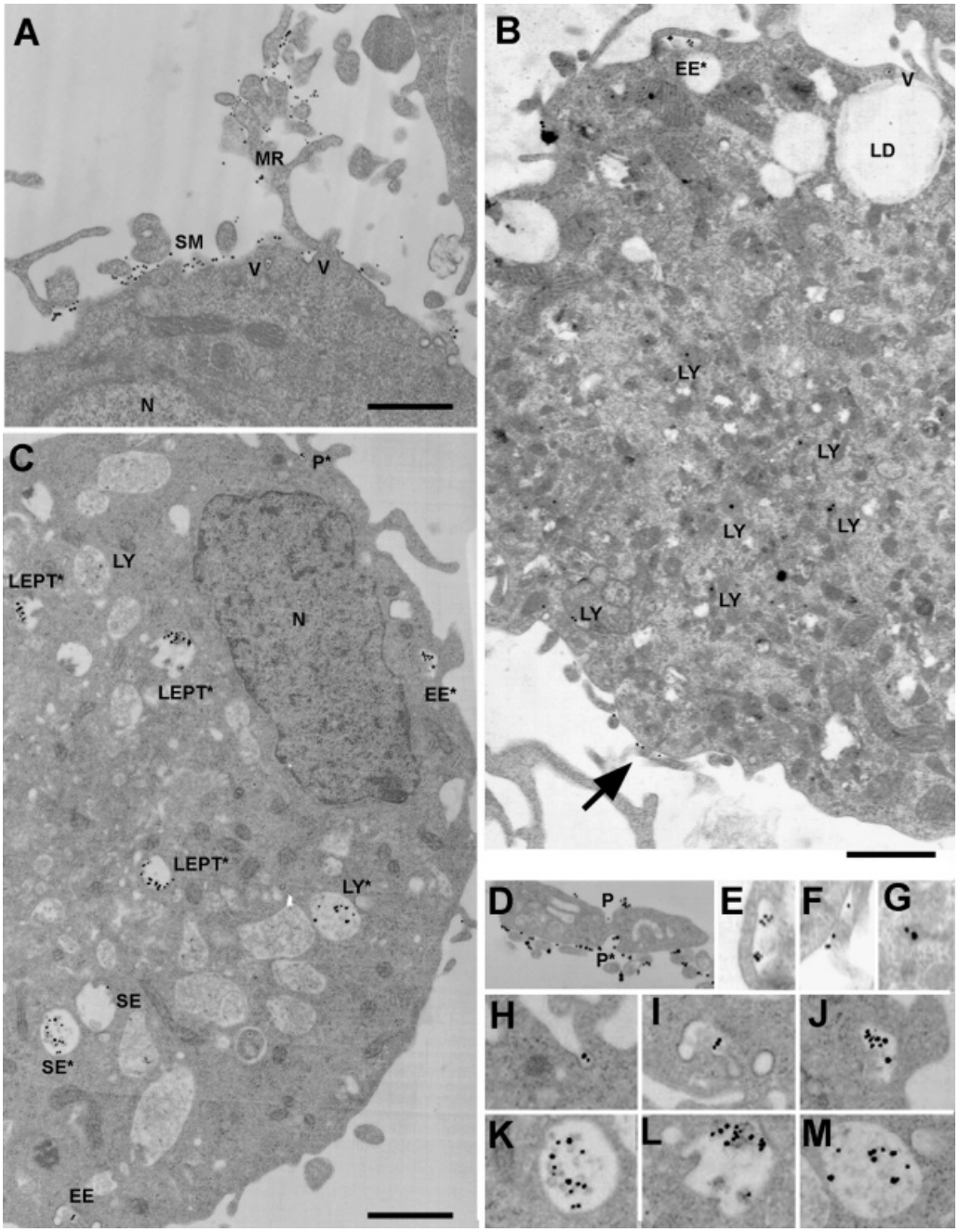


**Fig. 2.** Uptake of β-VLDL and LDL at high lipoprotein concentrations. Macrophages were incubated with β-VLDL and LDL at 50–100 μg/ml to examine uptake of lipoproteins at concentrations associated with in vitro foam cell formation. Cells were washed to remove nonbound lipoproteins and incubated at 37°C for <1, 5, 10, 30, 60, and 120 min. After fixation, the cells were examined by standard thin-section TEM. The micrographs are from three different experiments involving high concentrations of β-VLDL and LDL. The colloidal gold sizes were switched to control for steric effects. (A and H) β-VLDL-30 nm and LDL-16 nm for 5 min at 37°C; (B, E, F, and G) β-VLDL-21 nm and LDL-32 nm for 10 min at 37°C; (C, H–M) β-VLDL-30 nm and LDL-14 nm for 30 min at 37°C; (D) β-VLDL-21 nm and LDL-32 nm for <1 min at 37°C. Magnification bar: 1 μm. At early times, <1 min (D) and 5 min (A and H), both lipoproteins (both sizes of colloidal gold) are found in clathrin-coated pits (P) and vesicular profiles (V). At higher concentrations much lipoprotein is found on membrane ruffles (MR) and smooth portions of the plasma membrane (SM). (B, E–G) By 10 min, more LDL (small gold) than β-VLDL (large gold) is found in lysosomes [LY and (G)], while more β-VLDL is on the plasma membrane [arrow and (F)] and in early endosomes [EE and (E)] and vesicular profiles (V). At 30 min, β-VLDL and LDL are seen in most of the organelles associated with coated-pit endocytosis, clathrin-coated pits [P and (H)], and early endosomes [EE and (I) and (J)].

### Uptake of lipoproteins at concentrations that induce foam cell formation (high concentration)

Several differences were seen in the trafficking of β-VLDL versus LDL at high concentrations (**Fig. 2**). At 50–100 μg/ml, 13% more β-VLDL than LDL was retained on the plasma membrane at 10, 30, and 60 min. Conversely, 13% more of LDL than β-VLDL was in the lysosome at 10 and 30 min (Fig. 1). β-VLDL and LDL, coincubated at high concentrations, were maximally distributed to the pits and vesicular profiles and early endosomes by 5 min. LDL was maximally distributed to spherical endosomes by 10 min, but remained elevated through 60 min. β-VLDL was maximally distributed to spherical endosomes at 30 min, later than LDL. The distribution of both β-VLDL and LDL in the LEPT peaked at 60 min.

Only temporal differences were noted in trafficking of β-VLDL and LDL at high versus low concentrations. β-VLDL or LDL did not traffic significantly to other organelles such as macropinosomes. β-VLDL was delayed by 20 min to the spherical endosomes with maximal distribution at 30 min. Also, greater proportions of both lipoproteins were seen in spherical endosomes and LEPT at 30 and 60 min as compared with trafficking at lower concentrations. This could be accounted for by later entry from the plasma membrane and/or a longer retention time in these organelles.

### Colabeling of endocytic organelles

Experiments using the simultaneous incubation of lipoproteins were designed to detect if lipoproteins trafficked through the same endocytic organelles or if separate pathways were occurring during lipoprotein uptake. The percentage of each lipoprotein in the colabeled organelles was determined for β-VLDL and LDL. The extent of cotrafficking of β-VLDL compared with LDL was the same within each organelle at both low and high concentrations (**Fig. 3**). Pits and vesicular profiles had less than 10% colabeling, for LDL and β-VLDL, which was lower than in the rest of the endocytic pathway. The rest of the coated-pit endocytic organelles, early endosomes, spherical endosomes, LEPT, and lysosomes had on average 55% of β-VLDL and LDL cotrafficked in these organelles. These data are consistent with a previous study using this methodology (5), and other data indicating early endosomes as the sites of fusion between multiple vesicles; by that mechanism the lipoproteins are joined and exhibit consistently higher colabeling (17–20).

The extent of cotrafficking within any organelle type was not different between low and high concentrations. These data indicate that LDL and β-VLDL traffic through the same endocytic pathway and that there was not an additional atherogenic endocytic pathway at high β-VLDL concentrations. At high concentrations, however, the colabeling of LDL in LEPT was significantly greater than colabeling of LDL in the lysosomes. These data suggest that sorting of LDL occurs in the LEPT to different lysosomes. β-VLDL had a similar trend of a reduction in the extent of colabeling in lysosomes, but was not significantly different.

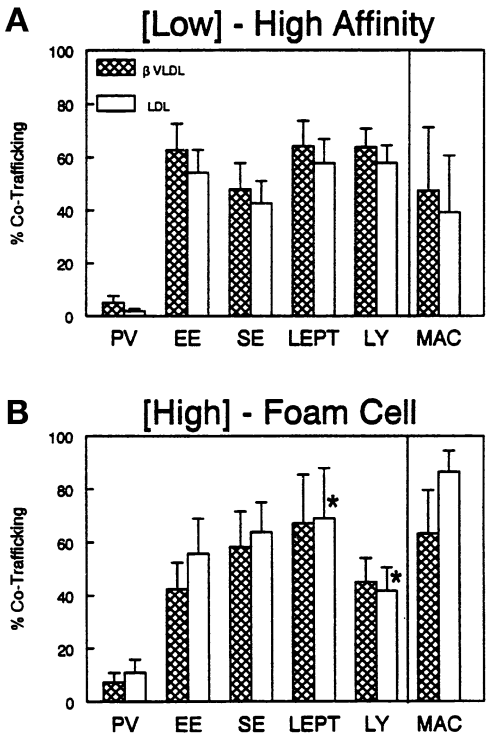


**Fig. 3.** The percentage of lipoprotein in colabeled organelles. The percentage of lipoprotein in colabeled organelles is shown for β-VLDL + LDL. (A) High affinity, low concentrations; and (B) Foam cells, high concentrations of lipoproteins. Colabeling was determined for the following organelles: clathrin-coated pits and vesicular profiles (PV), early endosomes (EE), spherical endosomes (SE), late endosomal-prelysosomal tubuloreticular compartment (LEPT), lysosomes (LY), and macropinosomes (MAC). Asterisks designate a significant difference at the $P < 0.05$ level between the percent colabeling of LDL in LEPT versus lysosomes at high concentrations of lipoproteins.

Previously, LEPT have been suggested as a site of organelle fusion and sorting (21).

### Lipoprotein-binding sites

Previously, pigeon β-VLDL binding at low concentrations or the high affinity binding sites were shown to be associated with distinct plasma membrane structures: microvilli and membrane ruffles (12, 16). To determine if distinct plasma membrane structures were associated with each lipoprotein, the plasma membrane-binding distribution for β-VLDL and LDL was quantified for the 10-min time points of the simultaneous trafficking experiments. At low concentrations, microvilli and membrane ruffles were the binding site for LDL and β-VLDL. Approximately 65% of β-VLDL and 47% of LDL bound to microvilli, while microvilli accounted for only 36% of the surface area of the cell (**Fig. 4**). About 20% of β-VLDL bound to both membrane ruffles and 16% bound to the smooth portions of the membrane, whereas 33% of LDL bound to membrane ruffles and 20% bound to the smooth portions of the membrane (Fig. 4). Although the distributions of β-VLDL and LDL are similar between membrane ruffles and smooth membrane, the membrane ruffle surface area was less than one-

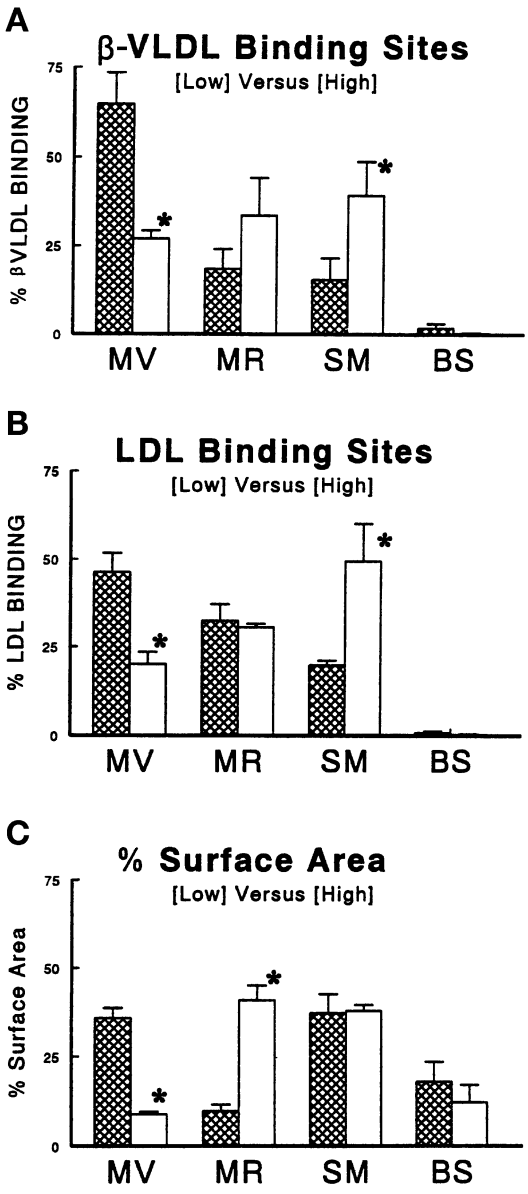


**Fig. 4.** Lipoprotein-binding sites and plasma membrane structure surface area. The 10-min time points from the simultaneous cotrafficking experiments were quantified for the percentage of lipoprotein binding to cell surface structures and the percentage surface area for each cell surface structure (Materials and Methods). The cell surface was divided into four categories: MV, microvilli and small ruffles (<0.22-m base width); MR, large membrane ruffles (>0.22-m base width); SM, smooth membrane regions; BS, basal surface. The percentage of lipoprotein binding was determined for (A) β-VLDL, (B) LDL, and (C) percentage surface area at low (cross-hatched columns) versus high (open columns) lipoprotein concentrations. Asterisks show a significant difference between the low and high concentrations at the $P < 0.05$ level.

third that of the smooth membrane surface area, indicating an enhancement of binding to membrane ruffles. The binding sites associated with the high affinity binding of β-VLDL and LDL were microvilli and, to a lesser degree, membrane ruffles.

Macrophages incubated with high concentrations of lipoproteins show binding to high affinity sites and low affinity sites. The plasma membrane surface area changes with incubation of high concentrations of lipoproteins. The plasma membrane surface had more membrane ruffles and less microvilli. The overall binding to microvilli for LDL and β-VLDL was lower with 20% and 27%, respectively, but the binding was enhanced because of the lower percent surface area of microvilli (Fig. 4). At high lipoprotein concentrations, LDL and β-VLDL binding shifted to binding on the smooth portion of the membrane, with 40% of β-VLDL and 50% of LDL. Comparison between high and low concentrations showed a reduction of binding to microvilli and an increase in binding to the smooth membrane. This shift toward binding on the smooth membrane correlated with lipoprotein low affinity or nonspecific binding sites on the macrophage. Consistent with this conclusion is the fact that rabbit β-VLDL and pigeon HDL, which have only low affinity binding sites (22), compete with pigeon β-VLDL binding to only membrane ruffles and smooth membrane, but not microvilli. In contrast, pigeon β-VLDL and LDL decreased pigeon β-VLDL binding to all three membrane structures (data not shown).

### Trafficking in macropinosomes

At higher concentrations of lipoprotein, a greater proportion of the surface area was membrane ruffles (Fig. 4C). Previously, we have shown that the extent of membrane ruffling directly correlates with the formation of macropinosomes (6). Although some macropinosomes were seen in macrophages, the overall distribution of lipoprotein in macropinosomes was low over the whole time course (Fig. 1 and **Fig. 5**). This was in contrast to trafficking of AcLDL, where half the lipoprotein trafficked in macropinosomes (6). Even when macropinosomes were present, the predominant intracellular sites for LDL and β-VLDL were in organelles consistent with coated-pit endocytosis: coated vesicular profiles, early endosomes, and spherical endosomes (Fig. 5). The distribution and the degree of colabeling for both β-VLDL and LDL increased at higher lipoprotein concentrations in macropinosomes (Figs. 1 and 3). The colabeling of LDL rose from 39% to 86%, which was significantly different. Colabeling of β-VLDL in macropinosomes had a similar trend from 48% to 63%. At higher concentrations, the greater distribution of β-VLDL and LDL and the greater colabeling most likely reflect a nonreceptor-dependent uptake. This would be consistent with entry of the lipoproteins into macropinosomes related to the concentration or fluid-phase uptake. Uptake of either LDL or β-VLDL via macropinocytosis was not the main internalization route; rather, organelles consistent with coated-pit endocytosis was the main internalization route.

## DISCUSSION

The hypothesis that intracellular processing of lipoproteins that stimulate cholesteryl ester accumulation and subsequent foam cell formation is different from the processing of those lipoproteins that do not cause foam cell formation has been explored. At concentrations of lipo-

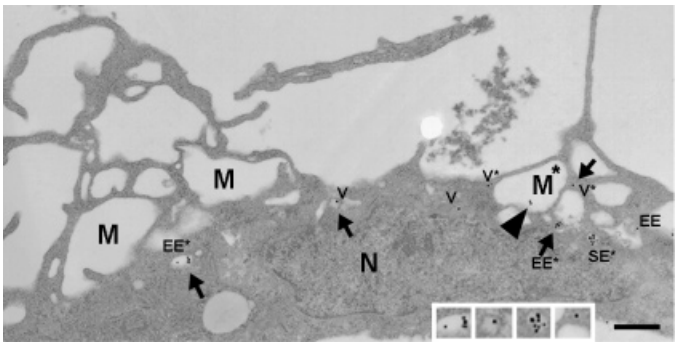


**Fig. 5.** Lipoprotein uptake not associated with macropinosomes. Macrophages were incubated with β-VLDL-21 nm and LDL-32 nm at 50–100 μg/ml to examine uptake of lipoproteins at concentrations associated with in vitro foam cell formation. Cells were washed to remove nonbound lipoproteins and incubated at 37°C for 5 min. Although, at high lipoprotein concentrations, an increase in membrane ruffling and formation of macropinosomes was seen compared with low lipoprotein concentrations, β-VLDL and LDL were rarely present in macropinosomes (M). Rather, β-VLDL and LDL were present in vesicular profiles (V), early endosomes (EE), and spherical endosomes (SE). The asterisks indicate cotrafficking of β-VLDL (small gold) and LDL (large gold). N, Nucleus. Magnification bar: 0.5 μm.

proteins near the saturation of high affinity binding, the predominant uptake is via coated-pit endocytosis for both this study and previous studies (5, 15). Differences in trafficking occurred when the concentrations of lipoproteins were above the saturation of the high affinity binding sites. For β-VLDL, uptake at concentrations attributed to foam cell formation was consistent with prolonged retention of lipoproteins on the plasma membrane, an increased binding to nonmicrovilli structures, and delayed or longer trafficking through organelles of the coated-pit endocytic pathway.

At low concentrations, the time courses of β-VLDL and LDL trafficking were similar to each other and to trafficking of each alone. The internalization was consistent with coated-pit endocytosis. When β-VLDL and LDL were incubated simultaneously, the same distribution and extent of cotrafficking were seen in all the organelles of coated-pit endocytosis: pits and vesicular profiles, early endosomes, spherical endosomes, LEPT, and lysosomes. This indicated that there was not a separate pathway associated with β-VLDL trafficking. At low concentrations, the surface structures associated with β-VLDL and LDL binding were microvilli and membrane ruffles. Previously, these structures have been associated with clathrin-coated pits (5, 16). LDL low density lipoprotein related receptors are on microvilli and membrane ruffles (23). The high affinity binding site for β-VLDL is the LDL receptor (23, 24).

Previously, trafficking of mammalian β-VLDL and LDL, at low concentrations, was shown to have temporal differences with β-VLDL internalized through unique structures called STEMs (10). No STEMs were seen in pigeon monocyte-derived macrophages internalizing pigeon β-VLDL at either low or high lipoprotein concentrations. The previously reported mammalian β-VLDL trafficking could be changed to an LDL trafficking pattern by pretreatment of β-VLDL with antibodies against apoE (25). Tabas et al. (25) suggest the localization to STEMs is due to multivalency of apoE and subsequent cross-linking of receptors. Pigeon β-VLDL does not have apoE (14). These studies also suggested that the presence of apoE and/or multiple apolipoprotein interactions with receptors may be necessary to stimulate the STEM structures, and without apoE, pigeon β-VLDL trafficked like pigeon LDL.

At high concentrations of β-VLDL and LDL, a greater proportion of the plasma membrane had membrane ruffles. Previously, a direct correlation between the extent of membrane ruffling and formation of macropinosomes was shown (6). Modified LDLs stimulate membrane ruffling and macropinocytosis resulting in uptake of modified LDLs by macropinocytosis. Potentially, β-VLDL and LDL at high concentrations could be internalized via macropinocytosis. However, no significant uptake of β-VLDL and LDL occurred by macropinocytosis.

Pigeon β-VLDL binds to macrophages by high affinity, low capacity receptors and low affinity, high capacity receptors and/or nonspecific processes. At low lipoprotein concentrations, 4°C binding, studies show the nonspecific binding component is minimal. However, at a β-VLDL concentration of 50–100 μg/ml a greater proportion of lipoprotein binding is low affinity and nonspecific (22). Pigeon β-VLDL binding to the low affinity site and subsequent internalization and degradation are mediated by cell surface heparan sulfate proteoglycans (HSPG)(24). In this study, at higher concentrations, the binding for LDL and β-VLDL shifted from microvilli to smooth membrane. The shift of binding from microvilli to smooth portions of the membrane most likely represents a shift in the proportion of the lipoprotein binding via the high affinity to the low affinity HSPG-binding sites. Competition of gold-conjugated pigeon β-VLDL supports this conclusion. Pigeon LDL, with only a high affinity binding site, blocked pigeon β-VLDL binding to microvilli. Rabbit β-VLDL, with only a low affinity HSPG-binding site (24), blocked binding to membrane ruffles and smooth membranes, but not microvilli. The decrease in lipoprotein binding to microvilli and increase in binding to the smooth membrane at high lipoprotein concentrations most likely represent a shift from primarily LDL receptor-binding sites to the low affinity HSPG-binding sites.

The mechanism of β-VLDL causing foam cell formation could be related to this increase in the proportion of β-VLDL binding to the low affinity binding site. Only at high concentrations, at which a greater proportion of β-VLDL bound to the low affinity binding sites, were differences in trafficking detected. The greater ability of rabbit β-VLDL to stimulate cholesterol accumulation was suggested to be due to binding to HSPG (24). Potentially, the HSPG-binding site of pigeon β-VLDL is largely responsible for uptake resulting in foam cell formation. Seo and St. Clair speculated that β-VLDL could be internalized via binding to proteoglycans without a transfer to the high af-

finity receptors (24). Whether transfer to high affinity receptors occurs is not known. Lipoproteins bound to HSPG might be internalized via membrane internalization rather than transferred to the high affinity receptors. In our system, at high concentrations, some macropinocytosis was stimulated. Therefore, a greater uptake of β-VLDL via macropinocytosis (larger portions of membrane internalization) would have been expected if HSPG internalization is related to membrane internalization. This was not seen; rather, most of the internalization was consistent with coated-pit endocytosis. This suggests that transfer to the high affinity receptors is necessary for internalization or that HSPG-binding sites can be selectively internalized via clathrin-coated pits.

The retention of β-VLDL on the plasma membrane, rather than a separate internalization mechanism via low affinity binding sites, might be a mechanism for foam cell formation. The retention of lipoproteins on the plasma membrane was previously suggested as a potential mechanism for increasing ACAT stimulation (8, 26). Direct delivery of cholesterol or lipid to the plasma membrane has been proposed. A similar surface exchange has been proposed in reverse for cholesterol transport to the HDL particles (27). In addition, enzymes such as sphingomyelinase could destabilize the lipoproteins, facilitating release of cholesterol to the plasma membrane (28). The longer retained β-VLDL was shown to undergo partial catabolism at the cell surface in STEMs (10).

Another hypothesis for differential metabolism of lipoproteins is that atherogenic lipoproteins are sorted to an altered lysosomal structure. Previously, β-VLDL uptake was shown to stimulate five acid phosphatase-positive lysosome morphologies, one of which was associated with lipid droplets (29). The data in the present study refute completely separate lysosome populations. However, at high concentrations of lipoproteins, some sorting to different lysosomes occurred. At high concentrations, the extent of colabeling of LDL in the lysosomes was less than in the LEPT, from 69% to 42%. A similar trend was seen for β-VLDL, from 67% in the LEPT to 45% in the lysosomes. These data indicate some separation of LDL from β-VLDL to different lysosomes. The sorting to different lysosomes might have been due to the colloid gold particles, rather than to the lipoprotein component of the conjugate. Macrophages can sort macromolecules internalized by endocytosis by size. Uniform mixtures of different-sized dextrans delivered into lysosomes separated into distinct organelles containing only one dextran or the other. Thus, the dynamics of endosomes and lysosomes are sufficient to segregate macromolecules by size (30). However, segregation to separate lysosomes was not noted at low lipoprotein concentrations when two sizes of gold were present. Another explanation for trafficking of LDL and β-VLDL to separate lysosomes might be that LDL reached the lysosomes more rapidly at high concentrations. β-VLDL resided for longer periods of time in spherical endosomes and LEPT, and might not have been available for complete mixing with the coincubated LDL. Further studies will be necessary to determine the significance of lysosomal subpopulations to foam cell formation.

Differences in trafficking of LDL and β-VLDL occurred when the concentration of lipoproteins was above the saturation of the high affinity binding sites. It is possible that uptake by receptor-mediated coated-pit endocytosis does not result in foam cell formation; rather, low affinity binding of β-VLDL to HSPG mediates foam cell formation. β-VLDL uptake at concentrations attributed to foam cell formation was consistent with a shift of binding to low affinity binding sites, prolonged retention of lipoproteins on the plasma membrane, delayed or longer trafficking through organelles of the coated-pit endocytic pathway, and separate lysosomes.

National Institutes of Health grant HL-41990 supported this work. William A. Hooker and Marie K. Plyler contributed the bulk of the technical assistance in these studies. We also thank the MICROMED staff for EM technical assistance.

*Manuscript received 11 November 1999 and in revised form 3 April 2000.*

## REFERENCES

1. Brown, M. S., and J. L. Goldstein. 1983. Lipoprotein metabolism in the macrophage: implications for cholesterol deposition in atherosclerosis. *Annu. Rev. Biochem.* **52:** 223–261.
2. Yancey, P. G., and W. G. Jerome. 1998. Lysosomal sequestration of free and esterified cholesterol from oxidized low density lipoprotein in macrophages of different species [in process citation]. *J. Lipid Res.* **39:** 1349–1361.
3. Henson, D. A., R. W. St. Clair, and J. C. Lewis. 1989. Morphological characterization of beta-VLDL and acetylated-LDL binding and internalization by cultured pigeon monocytes. *Exp. Mol. Pathol.* **51:** 243–263.
4. Henson, D. A., R. W. St. Clair, and J. C. Lewis. 1989. beta-VLDL and acetylated-LDL binding to pigeon monocyte macrophages. *Atherosclerosis.* **78:** 47–60.
5. Jones, N. L. 1997. Simultaneous labeling of lipoprotein intracellular trafficking in pigeon monocyte-derived macrophages. *Am. J. Pathol.* **150:** 1113–1124.
6. Jones, N. L., and M. C. Willingham. 1999. Modified LDLs are internalized by macrophages in part via macropinocytosis. *Anat. Rec.* **255:** 57–68.
7. Van Lenten, B. J., and A. M. Fogelman. 1990. Processing of lipoproteins in human monocyte-macrophages. *J. Lipid Res.* **31:** 1455–1466.
8. Tabas, I., S. Lim, X. X. Xu, and F. R. Maxfield. 1990. Endocytosed beta-VLDL and LDL are delivered to different intracellular vesicles in mouse peritoneal macrophages. *J. Cell Biol.* **111:** 929–940.
9. Zha, X., I. Tabas, P. L. Leopold, N. L. Jones, and F. R. Maxfield. 1997. Evidence for prolonged cell-surface contact of acetyl-LDL before entry into macrophages. *Arterioscler. Thromb. Vasc. Biol.* **17:** 1421–1431.
10. Myers, J. N., I. Tabas, N. L. Jones, and F. R. Maxfield. 1993. Beta-very low density lipoprotein is sequestered in surface-connected tubules in mouse peritoneal macrophages. *J. Cell Biol.* **123:** 1389–1402.
11. Kruth, H. S., S. I. Skarlatos, K. Lilly, J. Chang, and I. Ifrim. 1995. Sequestration of acetylated LDL and cholesterol crystals by human monocyte-derived macrophages. *J. Cell Biol.* **129:** 133–145.
12. Jones, N. L., N. S. Allen, and J. C. Lewis. 1991. Beta VLDL uptake by pigeon monocyte-derived macrophages: correlation of binding dynamics with three-dimensional ultrastructure. *Cell. Motil. Cytoskeleton.* **19:** 139–151.
13. St. Clair, R. W., R. K. Randolph, M. P. Jokinen, T. B. Clarkson, and H. A. Barakat. 1986. Relationship of plasma lipoproteins and the monocyte-macrophage system to atherosclerosis severity in cholesterol-fed pigeons. *Arteriosclerosis.* **6:** 614–626.
14. Barakat, H. A., and R. W. St. Clair. 1985. Characterization of

plasma lipoproteins of grain- and cholesterol-fed White Carneau and Show Racer pigeons. *J. Lipid Res.* **26:** 1252–1268.
15. Jones, N. L., J. W. Reagan, and M. C. Willingham. 2000. The pathogenesis of foam cell formation: modified LDL stimulated uptake of co-incubated LDL via macropinocytosis. *Arterioscler. Thromb. Vasc. Biol.* **20:** 773–781.
16. Landers, S. C., N. L. Jones, A. S. Williams, and J. C. Lewis. 1993. Beta very low density lipoprotein and clathrin-coated vesicles colocalize to microvilli in pigeon monocyte-derived macrophages. *Am. J. Pathol.* **142:** 1668–1677.
17. Salzman, N. H., and F. R. Maxfield. 1988. Intracellular fusion of sequentially formed endocytic compartments. *J. Cell Biol.* **106:** 1083–1091.
18. Ward, D. M., D. P. Hackenyos, and J. Kaplan. 1990. Fusion of sequentially internalized vesicles in alveolar macrophages. *J. Cell Biol.* **110:** 1013–1022.
19. Gruenberg, J., G. Griffiths, and K. E. Howell. 1989. Characterization of the early endosome and putative endocytic carrier vesicles in vivo and with an assay of vesicle fusion in vitro. *J. Cell Biol.* **108:** 1301–1316.
20. Dunn, K. W., and F. R. Maxfield. 1992. Delivery of ligands from sorting endosomes to late endosomes occurs by maturation of sorting endosomes. *J. Cell Biol.* **117:** 301–310.
21. Rabinowitz, S., H. Horstmann, S. Gordon, and G. Griffiths. 1992. Immunocytochemical characterization of the endocytic and phagolysosomal compartments in peritoneal macrophages. *J. Cell Biol.* **116:** 95–112.
22. Adelman, S. J., and R. W. St. Clair. 1988. Lipoprotein metabolism by macrophages from atherosclerosis-susceptible White Carneau and resistant Show Racer pigeons. *J. Lipid. Res.* **29:** 643–656.
23. Jones, N. L., M. Gupta, and J. C. Lewis. 1995. The LDL receptor and LRP are receptors for beta VLDL on pigeon monocyte-derived macrophages. *Virchows Arch.* **426:** 189–198.
24. Seo, T., and R. W. St. Clair. 1997. Heparan sulfate proteoglycans mediate internalization and degradation of beta-VLDL and promote cholesterol accumulation by pigeon macrophages. *J. Lipid Res.* **38:** 765–779.
25. Tabas, I., J. N. Myers, T. L. Innerarity, X. X. Xu, K. Arnold, J. Boyles, and F. R. Maxfield. 1991. The influence of particle size and multiple apoprotein E-receptor interactions on the endocytic targeting of beta-VLDL in mouse peritoneal macrophages. *J. Cell Biol.* **115:** 1547–1560.
26. Tabas, I. 1995. The stimulation of the cholesterol esterification pathway by atherogenic lipoproteins in macrophages. *Curr. Opin. Lipidol.* **6:** 260–268.
27. Johnson, W. J., F. H. Mahlberg, G. H. Rothblat, and M. C. Phillips. 1991. Cholesterol transport between cells and high-density lipoproteins. *Biochim. Biophys. Acta.* **1085:** 273–298.
28. Schissel, S. L., E. H. Schuchman, K. J. Williams, and I. Tabas. 1996. Zn2+-stimulated sphingomyelinase is secreted by many cell types and is a product of the acid sphingomyelinase gene. *J. Biol. Chem.* **271:** 18431–18436.
29. Jones, N. L., W. G. Jerome, and J. C. Lewis. 1991. Pigeon monocyte/macrophage lysosomes during beta VLDL uptake. Induction of acid phosphatase activity. A model for complex arterial lysosomes. *Am. J. Pathol.* **139:** 383–392.
30. Berthiaume, E. P., C. Medina, and J. A. Swanson. 1995. Molecular size-fractionation during endocytosis in macrophages. *J. Cell. Biol.* **129:** 989–998.